Mix Design and Properties of Recycled Aggregate Concretes: Applicability of Eurocode 2

George Wardeh, Elhem Ghorbel, Hector Gomart

International Journal of Concrete Structures and Materials
Vol.9, No.1, pp.1–20, March 2015
DOI 10.1007/s40069-014-0087-y
ISSN 1976-0485 / eISSN 2234-1315

Mix Design and Properties of Recycled Aggregate Concretes: Applicability of Eurocode 2

George Wardeh*, Elhem Ghorbel, and Hector Gomart

(Received May 23, 2014, Accepted July 24, 2014, Published online August 26, 2014)

Abstract: This work is devoted to the study of fresh and hardened properties of concrete containing recycled gravel. Four formulations were studied, the concrete of reference and three concretes containing recycled gravel with 30, 65 and 100 % replacement ratios. All materials were formulated on the basis of S4 class of flowability and a target C35 class of compressive strength according to the standard EN 206-1. The paper first presents the mix design method which was based on the optimization of cementitious paste and granular skeleton, then discusses experimental results. The results show that the elastic modulus and the tensile strength decrease while the peak strain in compression increases. Correlation with the water porosity is also established. The validity of analytical expressions proposed by Eurocode 2 is also discussed. The obtained results, together with results from the literature, show that these relationships do not predict adequately the mechanical properties as well as the stress–strain curve of tested materials. New expressions were established to predict the elastic modulus and the peak strain from the compressive strength of natural concrete. It was found that the proposed relationship E–f_c is applicable for any type of concrete while the effect of substitution has to be introduced into the stress–strain (ε_{c1}–f_c) relationship for recycled aggregate concrete. For the full stress–strain curve, the model of Carreira and Chu seems more adequate.

Keywords: recycled aggregate concrete, mix design method, mechanical properties, Eurocode 2.

1. Introduction

Aggregates consumption does not cease to grow in France. According to the UNPG (French national union of aggregates producers) and the UNICEM (French national union of industries of careers and building materials) aggregate production is estimated at 431 million tons in 2008, of which 79 % is used in civil engineering field and 21 % for building industry. In addition, 5 % of this amount is produced by recycling demolition wastes. Although this percentage remains low, recycling helps to limit the environmental impact by limiting the exploitation of natural resources. These socio-economic issues are the driving forces promoting the recycled aggregates in concrete.

The valorization of recycled aggregates in concrete is not recent and many studies have shown that material made with recycled aggregates may have mechanical properties similar to those of a conventional concrete mixed with natural aggregates (Etxeberria et al. 2007; Evangelista and de Brito 2007; Li 2008; McNeil and Kang 2013). However, recycled aggregates are characterized by a high water absorption capacity related to the presence of old mortar attached to the surface of aggregates which hinders their wide use (Gomez-Soberon 2002; de Juan and Gutirrez 2009). The water absorption capacity affects both fresh and hardened states properties. At fresh state, the mix design of concrete with recycled aggregates requires an additional quantity of water to obtain a similar workability as a concrete formulated with natural aggregates (Hansen and Boegh 1986). Such a modification may obviously affect the mechanical characteristics of recycled aggregates concrete. Several studies have investigated the microstructure of recycled aggregates concrete and showed that the porosity is modified and increases with the replacement ratio (Gomez-Soberon 2002). It is also acknowledged that the high porosity of recycled concrete leads a reduction of the mechanical strengths (Gomez-Soberon 2002; Kou et al. 2011). Furthermore, several studies have shown however that mechanical properties of concrete made with recycled aggregates depend on other parameters such as the quality of concrete from which recycled aggregates are obtained (Xiao et al. 2005; Casuccio et al. 2008) as well as the replacement ratio (Belén et al. 2011).

The main goal of this work is to determine the properties of recycled aggregate concretes (RAC) at fresh and hardened states depending on replacement ratio. A concrete made with natural aggregate (NAC), designed for control operations, and three RAC with a S4 class of workability and compressive strength levels near to 35 MPa were formulated and tested. The present study also examines the applicability of relationships of Eurocode 2 (EC2) to concretes made from recycled aggregates. These relationships estimate the modulus of elasticity, the peak strain and stress–strain relationship from the simple knowledge of the compressive strength.

University of Cergy-Pontoise, Neuville-sur-Oise 95031, France.
*Corresponding Author; E-mail: george.wardeh@u-cergy.fr

2. Materials

2.1 Cement

CEM I CALCIA 52.5 N CE CP2 NF cement in conformity with the standard EN 197-2 was used in all concrete mixes. The chemical and mineralogical compositions calculated by the method of Bogue are presented in Table 1. The density of this cement is 3.11, its Blaine surface is 395 (m^2/kg) and its compressive strength after 2 days is 31.7 (MPa).

2.2 Aggregates

The fine aggregates are 0/4 mm silico-calcareos rolled sand. For all mix designs, two size fractions of coarse natural crushed silico-calcareos aggregates were used. The particles size of the first fraction, called G_1, is comprised between 5 and 10 mm while it is comprised between 10 and 20 mm for the second type G_2. Recycled aggregates were delivered in big bags from a retreatment platform of demolition materials. They were sieved in the laboratory into three fractions GR_1 (4/10 mm), GR_2 (10/20 mm) and sand (0/5 mm). In this study only the coarse recycled aggregates were used. They were dried in an oven at 110 ± 5 °C and then stocked in closed containers until the moment of concrete manufacture. The main properties of the natural and recycled aggregates are presented in Table 2 and the grading curves are plotted in Fig. 1. It is seen that the size grading of the coarse natural and recycled gravel was similar with a larger amount of small particles for GR_1.

Water absorption has been characterized first, according to the standard NF EN 1097-6 at the atmospheric pressure. Dried aggregates were immersed in water during 24 h then dried again in an oven at a temperature of 110 ± 5 °C. It can be noticed in Table 2 that recycled aggregates have a significant higher water absorption capacity and a lower density than natural ones. In spite of the high water absorption capacity of the used RCA, it remains within the range recommended by the design standards (McNeil and Kang 2013; Kang et al. 2014).

The kinetic of water absorption of recycled aggregates GR_1 and GR_2 was also followed and the water uptake was measured by hydrostatic weighting. Aggregates samples were washed first on the sieve of 4 mm and dried in an oven at a temperature of 110 ± 5 °C until mass stabilization. After drying the tested sample was placed between two stainless sieves (of diameter 15 cm and height 7 cm) for hydro-static weighing. The system was hung to a balance of 0.01 g accuracy with a non-elastic wire and the mass variation is continuously recorded. The room temperature is equal to 22 °C. Figure 2 illustrates the measurement system.

The water absorption was calculated according to the following equation:

$$\omega_a = \frac{M_{wa} - M_{ws}}{M_s} \times 100, \quad (1)$$

where M_{wa} is the mass of saturated aggregates in water at time t, M_{ws} is the mass of dried aggregates in water at t_0, and M_s is the mass of dried aggregates in air. The t_0 indicates the beginning of the test.

Figure 3 shows the evolution of water absorption versus time. At $t = 24$ h, water absorption of GR_1 and GR_2 are respectively equal to 8.3 and 6.5 %. These results correspond to the values obtained following NF EN 1097-6 standard (cf. Table 2). Results show also that recycled aggregates are saturated after a "long time" more than 24 h, according to several studies (Tam et al. 2008; Djerbi Tegguer 2012). At $t = 24$ h, water absorption represents only 82 and 85 % of total degree of saturation for GR_1 and GR_2, respectively. Finally, aggregates reach a water absorption of 10 and 7.8 % for GR_1 and GR_2, respectively. At the opposite, for short time relative to mixing time (5 min), the kinetic of absorption is fast.

2.3 Superplasticizer

The used Superplasticizer is Cimfluid 3002 produced by Axim Italcementi group with a solid content of 30 %. It is a new generation product based on chains of modified polycarboxylate certified in conformity with the standard EN 934-2 and considered as a water reducing admixture.

3. Mix Method and Concrete Proportions

All mixtures were formulated on the basis of the following specifications:

- only coarse natural aggregates are replaced by recycled ones with three volumetric replacement ratios 30, 65 and 100 %;
- the granular skeleton is constituted of a ternary mixture of sand and two gravels G_1 (4/10 mm) and G_2 (10/20 mm);
- at fresh state, all concretes are of S4 workability class where the target slump with the Abrams's cone is 18 ± 1 cm. According to the standard NF EN 206-1 the slump for a S4 flowability is comprised between 16 and 21 cm;
- at hardened state a compressive strength comprised between 35 and 43 MPa must be guaranteed at the age of 28 days;
- concretes are designated for XF2 class of environmental exposure according to the standard NF EN 206-1, where water to cement ratio (W/C) is lower than or equal 0.5 and the minimum cement content is higher than 300 kg/m^3.

Table 1 Chemical and mineralogical compositions of the used cement in %.

SiO_2	Al_2O_3	Fe_2O_3	CaO_{total}	MgO	SO_3	K_2O	Na_2O	C_3S	C_2S	C_3A	C_4AF
19.8	5.14	2.3	64.9	0.9	3.4	1.1	0.005	58	13	10	6.99

Table 2 Physical properties of used aggregates.

	Sand	G_1	G_2	GR_1	GR_2
Dry bulk density (kg/m^3)	2,550	2,510	2,510	2,240	2,240
Water absorption, ω_a (%)	1.7 ± 0.03	1.6 ± 0.07	1.8 ± 0.05	8.2 ± 0.5	6.5 ± 0.4
Fineness modulus	2.82	–	–	–	–

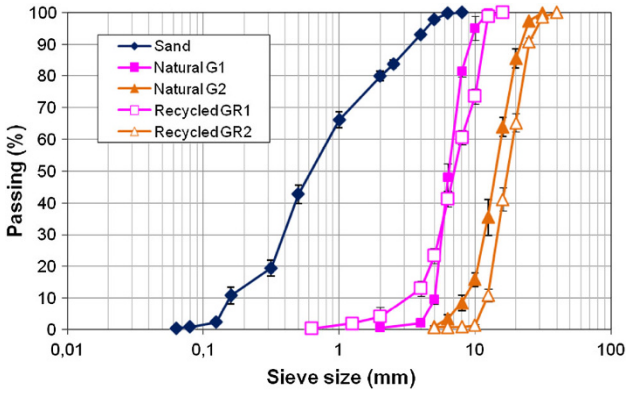

Fig. 1 Aggregate gradation curves.

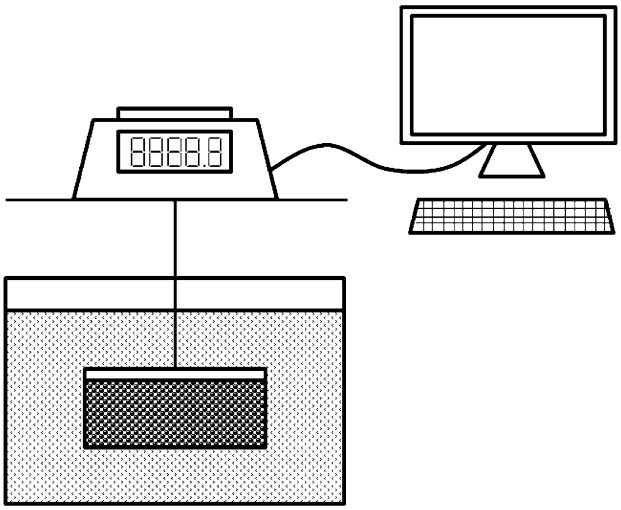

Fig. 2 Water absorption measurement system.

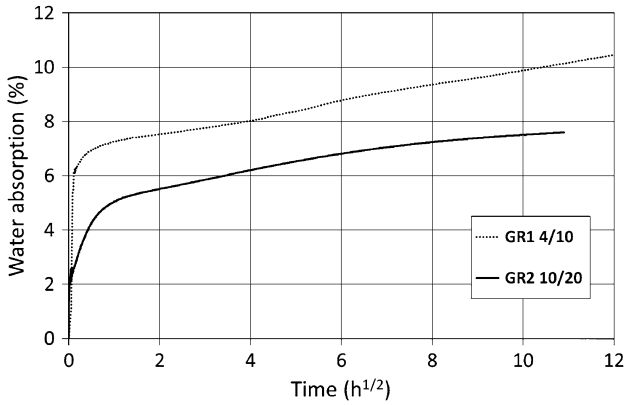

Fig. 3 Water absorption of recycled aggregates.

A total of four concretes were then produced, a mix with natural aggregates called (NAC) and three concretes with recycled aggregates named RAC30, RAC65 and RAC100. The numbers indicate the rate of substitution. For NAC the cement content is taken equal to 360 kg/m^3 according to the standard NF EN 206-1 while for the other mixes this content was modified as will be explained below.

3.1 Optimization of Water to Cement Ratio

The quantity of water for the cement was determined based on the flowability requirement by means of spread tests with the mini flow cone for which dimensions are 8 cm for lower diameter, 7 cm for upper diameter and 4 cm for the height (Fig. 4).

For various water/cement ratios the slump d_m and the relative slump Γ_m are computed using the following equation:

$$d_m = \frac{d_1 + d_2}{2};\ \Gamma_m = \frac{d_m^2 - d_0^2}{d_0^2}, \tag{2}$$

where d_0 is the lower diameter of the cone, d_m is the average of two wafer diameters d_1 and d_2. In Fig. 4 the relative slump Γ_m is depicted against the water to cement ratio, where a straight line fits the experimental results with a correlation ratio $R^2 = 0.99$. The relative slump $\Gamma_m = 5$ yields the water content necessary for a flowable paste (El-Hilali 2009).

3.2 Optimization of Solid Skeleton

Granular skeleton was optimized by the method of compaction using vibration. The study started by measuring the packing density of each component, i.e. sand, natural gravels G_1, G_2 and recycled gravels GR_1, GR_2. Binary mixtures of

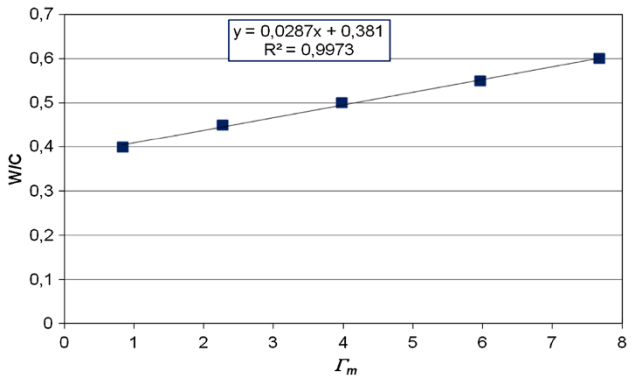

Fig. 4 Water to cement ratio versus relative slump.

gravel were then tested to determine optimal dosages which give the densest packing. Finally ternary mixtures were tested to optimize the solid skeleton for all mixes.

Packing tests were conducted according to the test method No. 61 of LCPC (Lédée et al. 2004). To determine the packing density of a given granular fraction, a sample is poured in 16 × 32 cm^2 cylindrical mold then vibrated while applying a pressure of 10 kPa. The packing density is calculated by the equation:

$$C = \frac{H_f}{H_i}, \tag{3}$$

where H_f is the sample height after vibration and H_i the height before vibration. The results for components are summarized in Table 3 where each value is the average of three measurements. From this table it can be noticed that the packing density of recycled aggregates is lower than that of natural aggregates due to the presence of old cement paste.

Optimal proportions of granular mixtures are reported in Table 4 where an increase in the sand content can be observed for recycled aggregates to assess the highest packing. This increase is due mainly to the lower density and lower packing ability of recycled aggregates.

Values of Table 4 were obtained by conducting packing tests on each mixture with several proportions. The curve representing the variation of packing density as a function of proportions was then plotted. The chosen optimal dosage is the point which corresponds to the maximum of the curve as shown in Fig. 5 for the ternary mixture of sand with recycled aggregates. For concretes RAC30, RAC65 the solid skeleton was first optimized where 30 and 65 % coarse natural aggregates were replaced by recycled aggregates GR_1 and GR_2 and the packing tests were conducted. The results showed that proportions sand to aggregates remain the same as for the mixture sand with recycled aggregates.

In order to corroborate the obtained experimental results, the software RENE LCPC was used (Sedran 1999). The software is able, from packing density and the size distribution curves of aggregates, to predict the packing density of a mixture. The results, plotted on Fig. 4, show that theoretical results are in tune with the experimental results.

3.3 Mix Proportions of all Components

Recycled aggregates have not been pre-saturated and the amount of absorbed water was added to the mixing water. Moreover, since the amount of water is important, an additional quantity of cement was added such that the ratio of total water to cement remains constant. For NAC, the dosage of superplasticizer was gradually increased until the target slump was obtained. This dosage has not been modified for the other formulations because water initially added to mixes had allowed to obtain the slump 18 ± 1 cm.

Table 5, containing the mixes, shows that the adopted approach leads to an increase in paste volume with a slight decrease in density. In this table, the effective water, W_{eff}, is defined according to the standard EN 206-1 as the total water quantity, W_{tot}, minus the water absorbed by aggregates $W_{\text{eff}} = W_{\text{tot}} - \omega_a \times M_{\text{g}}$ where M_{g} is the weight of dry aggregates.

Cylindrical 16 × 32 cm^2 specimens were prepared to determine the compressive strength, elastic modulus and splitting tensile strength. Furthermore plain and prenotched 10 × 10 × 40 cm^3 prismatic specimens were cast to determine the flexural strength of studied concretes. After being removed from the mold, they were cured in a water tank at room temperature for 28 days.

3.4 Test Methods

Uniaxial compression and tensile splitting tests were performed using a servo-hydraulic INSTRON machine with a capacity of 3,500 kN by imposing a stress increment rate of 0.5 MPa/s. Each test was repeated at least three times and results shown below are the averages of obtained values. In addition one cylinder of each material was instrumented with two strain gauges in order to determine the elastic modulus, and test were performed by imposing a strain rate of 1 mm/min. Bending tests were performed using a 250 kN closed loop INSTRON machine with a strain rate of 1 mm/min. Finally, splitting strength was measured using the Brazilian test and dynamic modulus of elasticity was determined using E-Meter MK II device.

Water porosity was determined using the vacuum saturation method. The test includes two stages, the first consists on submitting 10 × 10 × 10 cm specimens, dried at 60 ± 5 °C, to vacuum (about 80 mbar) during 3 h. After this period and in a second stage, specimens are immersed in water during 5 days. The water absorption, called water porosity, is determined as follows:

$$W_A = \frac{W_{\text{sat}} - W_{\text{dry}}}{W_{\text{sat}} - W_{\text{wat}}} \times 100, \tag{4}$$

with W_{sat} is the weight of the saturated sample, W_{dry} is the weight of the dry sample, W_{wat} is the weight of the saturated sample immersed in water.

4. Test Results

4.1 Properties of the Fresh Concretes

The results of workability tests and air content are given in Table 6 where it can be seen that all mixtures compile with the required workability. It can be concluded that the air

Table 3 Packing densities of used aggregates.

	Sand	Natural aggregates		Recycled aggregates	
		G_1	G_2	GR_1	GR_2
Packing density	0.894 ± 0.027	0.885 ± 0.002	0.886 ± 0.001	0.866 ± 0.002	0.875 ± 0.011

Table 4 Volumetric optimal proportions of mixes.

	NAC	RAC30	RAC65	RAC100
$\frac{S}{G_1+G_2}$	0.67	0.82	1.51	–
$\frac{G_1}{G_2}$	0.50	0.53	0.67	–
$\frac{S}{GR_1+GR_2}$	–	0.82	1.51	1.50
$\frac{GR_1}{GR_2}$	–	0.52	0.67	0.67

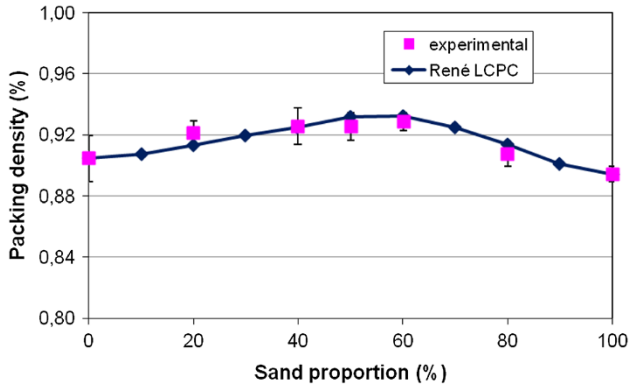

Fig. 5 Packing density of ternary mixture S + GR_1 + GR_2.

content of RAC is higher than concrete made with NA when the replacement ratio exceeds 30 %.

The slump loss during 2 h is plotted in Fig. 6 for all studied materials where the slump values are averages of two measurements. During the first 20 min, the loss is not significant for RAC65 and RAC100 and this is explained by the excess of available water in the mix. After 20 min the loss is more pronounced when the replacement ratio is higher. This trend was also observed by Poon et al. (2011).

In order to verify if the accentuation is due to the continuous water absorption by recycled aggregates and not to the increase in paste volume, the loss in workability of two cement pastes corresponding to NAC and RAC100 was followed during 2 h. Figure 7 shows the changes of paste slumps with time where it can be seen that the two pastes undergo the same kinetic of loss.

4.2 Properties of the Hardened Concrete Specimens

4.2.1 Water Porosity

Figure 8 presents the water porosities, measured at atmospheric pressure and under vacuum conditions, for all

Table 5 Mix proportions for 1 m^3.

	NAC	RAC30	RAC65	RAC100
Cement (kg/m^3)	360	360	427	448
Effective water, W_{eff} (kg/m^3)	180	180	180	180
Additional water, w_a (kg/m^3)	–	10	42	53
Sand (kg/m^3)	703	780	957	930
Natural aggregates G_1 (4/10 mm) (kg/m^3)	346	227	88	–
Natural aggregates G_2 (10/20 mm) (kg/m^3)	692	429	131	–
Recycled aggregates GR_1 (4/10 mm) (kg/m^3)	–	86	145	218
Recycled aggregates GR_2 (10/20 mm) (kg/m^3)	–	164	218	326
Superplasticizer (kg/m^3)	1.25	1.25	1.25	1.25
Effective water/cement (W_{eff}/C)	0.50	0.50	0.42	0.40
Total water/cement (W/C)	0.50	0.52	0.52	0.52
Paste volume (%)	29.6	30.6	36.0	37.8
Theoretical density (kg/m^3)	2,280	2,236	2,188	2,155
Experimental density (kg/m^3)	2,287 ± 3 %	2,224 ± 2 %	2,190 ± 1 %	2,159 ± 1 %

Table 6 Properties of fresh concrete mixes.

Mix	Slump (cm)	Air content (%)
NAC	18 ± 0.7	1.6 ± 0.3
RAC30	19.3 ± 1.5	1.8 ± 0.1
RAC65	18.5 ± 1.0	2.0 ± 0.2
RAC100	20 ± 1.4	2.5 ± 0.2

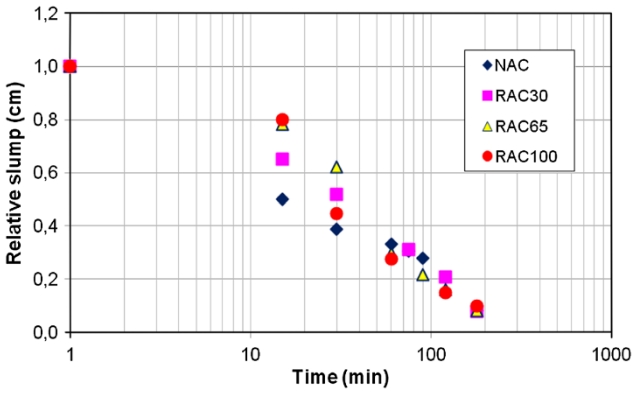

Fig. 6 Slump loss of concrete mixes with time.

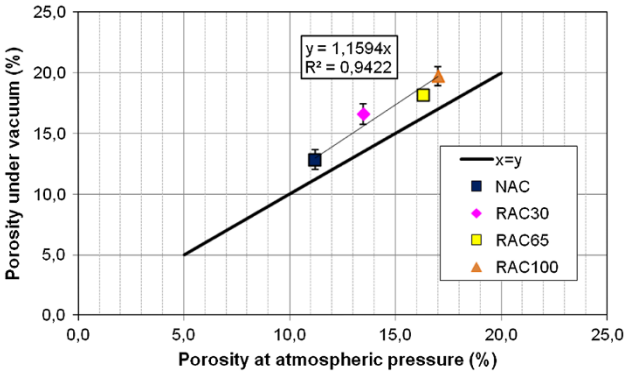

Fig. 8 Water porosities measured at atmospheric pressure and under vacuum.

concrete mixes. It can be pointed out that both porosities increase with replacement ratio. These results are in agreement with the results of the literature where the porosity increases with substitution rate (Gomez-Soberon 2002; Belin et al. 2013). It can be also shown that the ratio between the porosity measured under vacuum and the porosity measured at atmospheric pressure is constant and equal to 1.16.

The increase of porosity with replacement ratio is mainly due to the high porosity of recycled aggregates, to the increase in the paste volume and to the poor interface paste-aggregates as well as to the increase in air content (cf. Fig. 9).

4.2.2 Compressive Strength

Figure 10 shows compressive strength results at 7, 14, 21 and 28 days for the four concretes produced in this work. As illustrated in this figure, comparable strengths were obtained for all concretes with a decrease of 13 % for the concrete RAC30. This strength loss is due to recycled aggregates and to the increase in the total water quantity without correcting the cement content. For substitution ratio higher than 30 %, two phenomena are in competition: increasing the cement content and the replacement ratio of recycled aggregates which contribute to the increase of strength in the first case and the decrease in the second. However, the materials satisfy correctly the imposed specifications given in part 3 i.e. S4 flowability and 35 MPa compressive strength concretes.

Compressive strength results were compared to the Féret strength equation with 54 results found in references (Xiao et al. 2006; Etxeberria et al. 2007; Evangelista and de Brito 2007; Gomes and Brito 2009; Belén et al. 2011; Martinez-Lage et al. 2012; Pereira et al. 2012; Manzi et al. 2013). The Féret strength equation is:

$$\frac{f'_c}{f_{cm}} = K\left(\frac{v_c}{v_c + v_w + v_a}\right)^2, \quad (5)$$

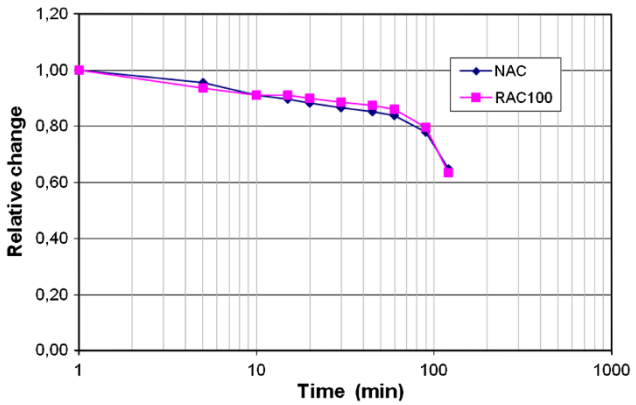

Fig. 7 Slump loss of cement pastes with time.

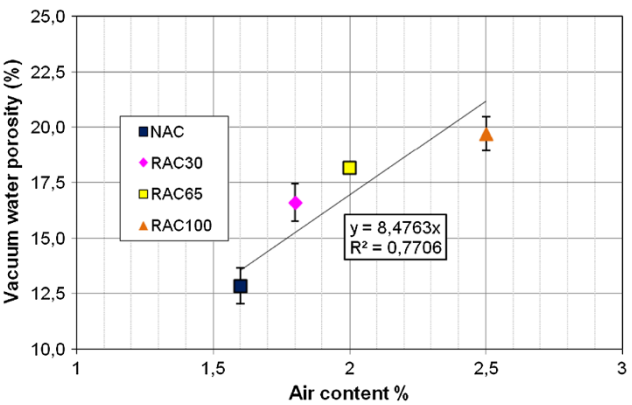

Fig. 9 Relationship between air content and water porosity.

where K is the Féret coefficient which depends on mix design and age, f_c' is the compressive strength of concrete (MPa), f_{cm} is the normal compressive strength of cement, v_c is cement content in concrete (m^3/m^3), v_w is the water content in concrete (m^3/m^3) and v_a is the air content in concrete (m^3/m^3).

The K value was evaluated based on the both natural and recycled aggregates concretes compressive strength (cf. Figure 11). It is found that a value of 5.27 fits adequately the experimental results with a correlation factor $R^2 = 0.7$. The obtained value is close to the theoretical value of $K = 5$ found in the literature (Julio et al. 2006; Hacene et al. 2009).

Féret's equation can therefore help to explain the obtained compressive strengths for RAC65 and RAC100. Indeed, at a constant W/C ratio, when the concentration of cement increases in the paste volume (i.e. the reduction of effective water to cement ratio), the compressive strength is maintained constant despite the increase in air content (Table 5).

Moreover, the compressive strength of RAC30 decreased due to the reduction in cement concentration in the cement paste.

4.2.3 Elastic Modulus

The variation of both static and dynamic modulus of elasticity, denoted E, at the age of 28 days is plotted in Fig. 12. It can be seen that the recycled aggregates have a significant effect on the elastic modulus where it decreases with the increase of replacement ratio. These results are in good agreement with the literature results which indicate a decrease in the elastic modulus (Xiao et al. 2006; Casuccio et al. 2008). This reduction is the consequence of the application of recycled aggregates with a higher porosity and a lower elastic modulus than those of the natural coarse aggregates.

4.2.4 Flexural and Splitting Tensile Strengths

The flexural strength obtained for all concretes is shown in Fig. 13 with the tensile splitting strength. It is possible to conclude that the tensile strength with recycled aggregates is negatively affected when replacement ratio increases. The loss of both flexural and tensile strengths is about 6 % for RAC30, 11 % for RAC65 and reaches 20 % for RAC100.

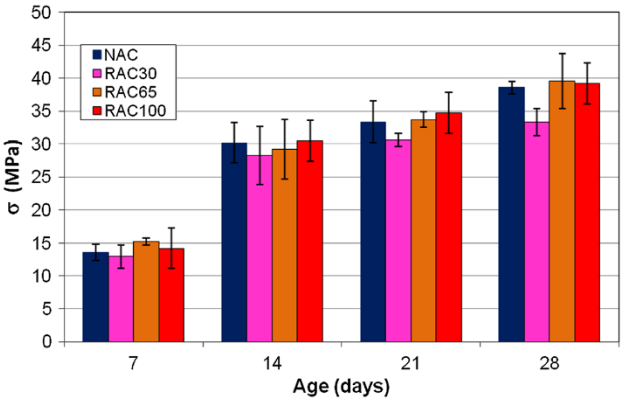

Fig. 10 Compressive strength as a function of age and replacement (means and standard errors).

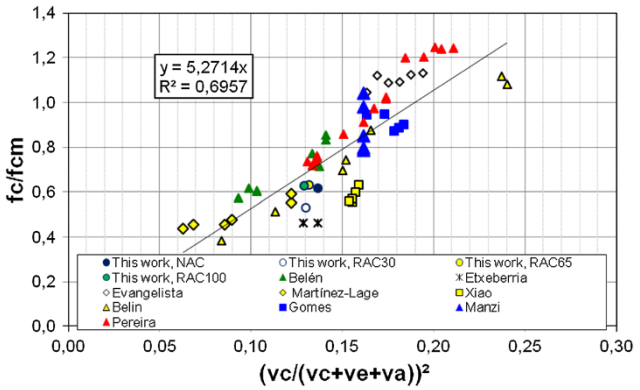

Fig. 11 Relationship between relative compressive strength and cement, water and air contents.

The correlation between tensile strength and the porosity is illustrated on Fig. 14. The results, as might be expected, show a decrease in tensile strength when the porosity increases. Figure 15 shows the normalized static modulus of elasticity versus the normalized tensile strength. The linear correlation indicates that the higher porosity of recycled aggregates affects both characteristics. These results are in agreement with those established by Evangelista and de Brito (2007).

4.2.5 Analysis of Peak Strain and Stress–Strain Relationship Under Compression

Stress–strain curves were obtained by uniaxial compressive tests for all materials developed in the present work. The analysis of these curves shows that the peak strain corresponding to the maximum stress increases when increasing the replacement ratio. The evolution of this strain, normalized by the strain of NAC, is shown in Fig. 16 as a function of the rate of substitution with the results of Belén et al. (2011) and Martínez-Lage et al. (2012). The results show a linear increase of the normalized peak strain with the replacement ratio. However, this increase is more significant in the context of our work and it is probably attributed to the adopted experimental conditions.

The influence of the recycled aggregates content on the complete stress–strain curves was also investigated. The results shown on Fig. 17 indicate that the shape of the post-

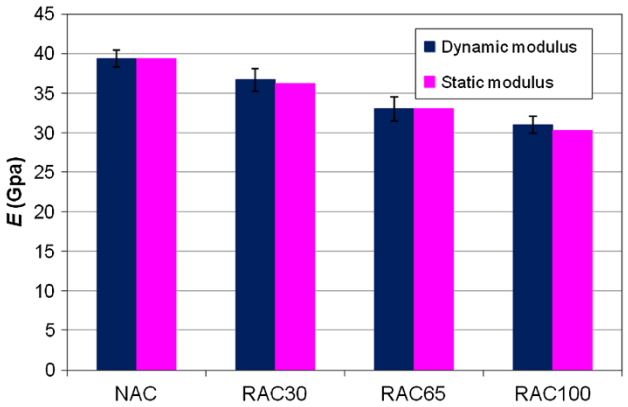

Fig. 12 Variation of modulus of elasticity as a function of replacement ratio.

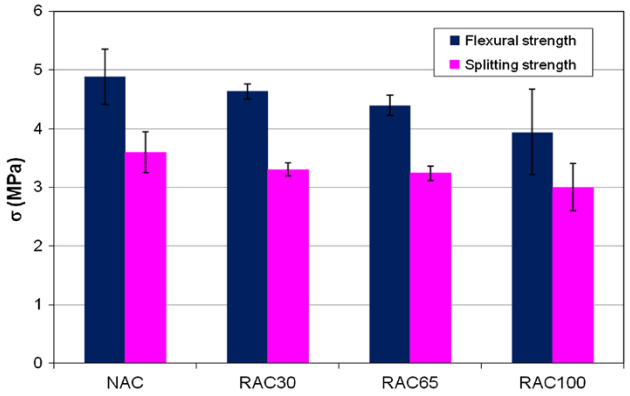

Fig. 13 Flexural and splitting strength as a function of replacement.

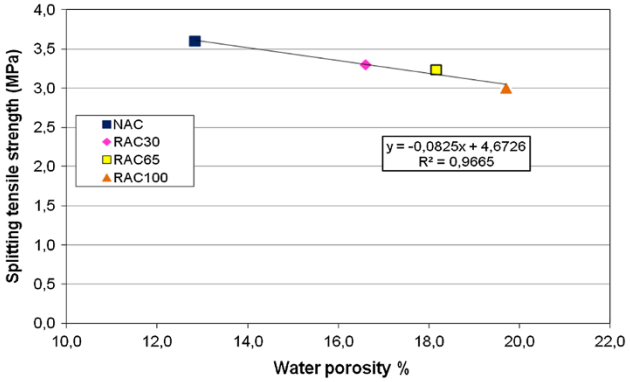

Fig. 14 Splitting tensile strength versus water porosity.

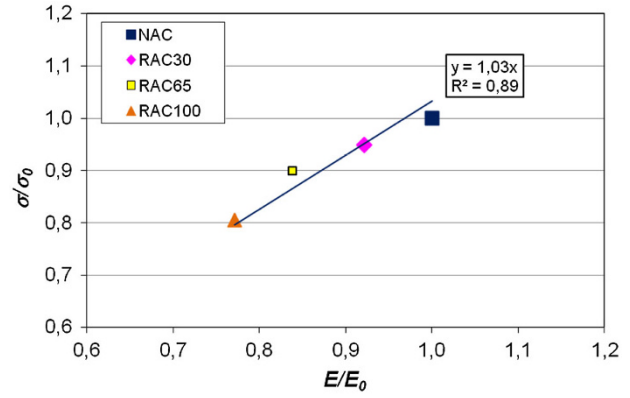

Fig. 15 Correlation between the elastic modulus and tensile strength.

peak curve is more spread when the replacement ratio is important. This observation highlights a more dissipative behavior when recycled aggregates are used, and may be explained by a more diffuse damage related to the nature of recycled aggregates.

5. Prediction of Stress–Strain Relationship and the Applicability of EC2

Eurocode 2 proposes the following expression for predicting elastic modulus E (in MPa) from compressive strength f_c' (in MPa).

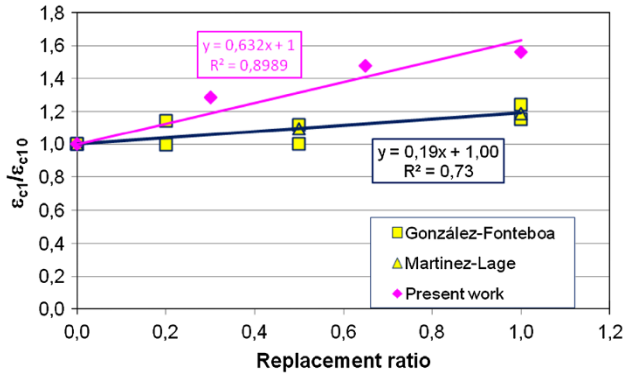

Fig. 16 Influence of RCA content on the peak strain.

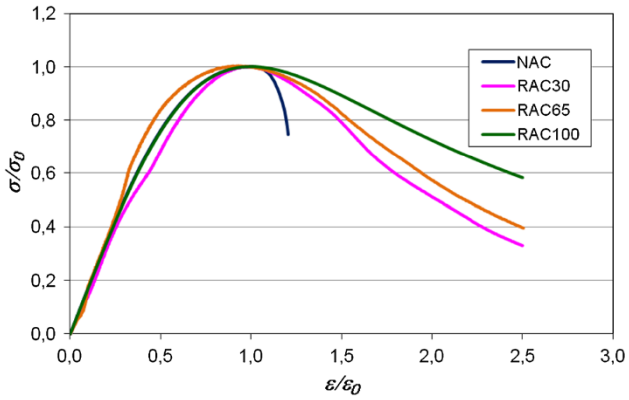

Fig. 17 Normalized stress–strain relationship.

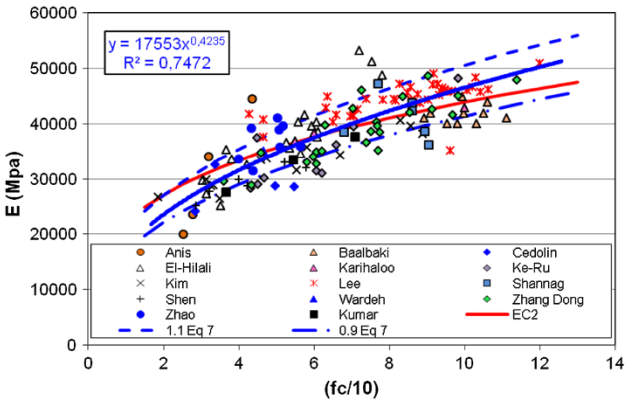

Fig. 18 Elastic modulus of NAC as a function of compressive strength.

$$E = 22000\left(\frac{f_c'}{10}\right)^{0.3}. \quad (6)$$

The validity of the previous expression was verified using more than 230 concretes formulated with natural aggregates (see Table 7 in "Appendix" section). The results are plotted in Fig. 18 and the data analysis shows that the expression of EC2 does not allow a satisfactory prediction of elastic modulus. Equation (6) fits experimental results with correlation factor $R^2 = 0.68$ while the proposed Eq. (7) provides a better description of the experimental results.

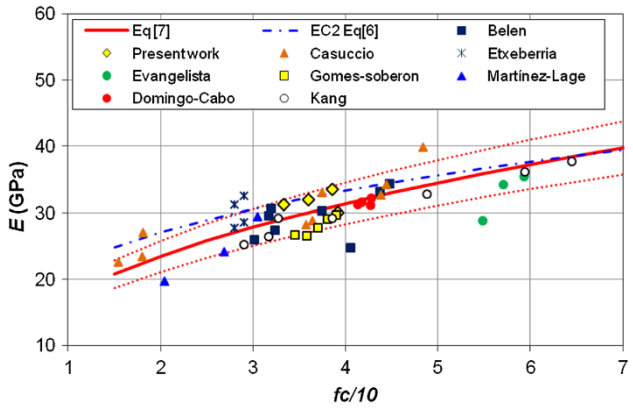

Fig. 19 Variation of modulus of elasticity of RAC as a function of compressive strength.

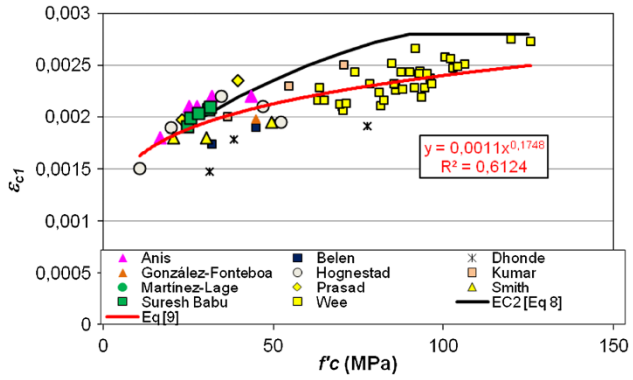

Fig. 20 Peak-strain as a function of compressive stress.

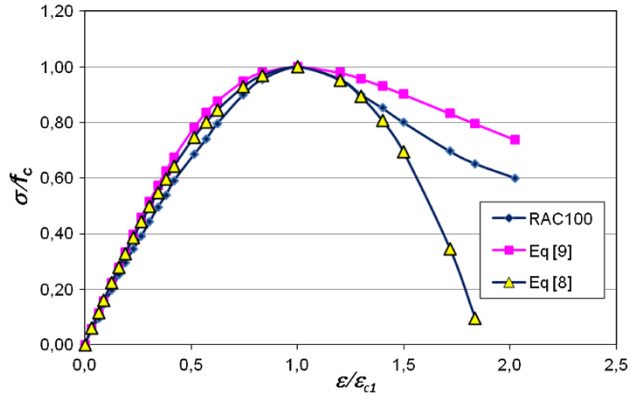

Fig. 21 Strain–stress curves.

$$E = 17553\left(\frac{f_c'}{10}\right)^{0.42}. \tag{7}$$

The elastic modulus of RAC developed in this work together with the results found in the literature (Gomez-Soberon 2002; Etxeberria et al. 2007; Evangelista and de Brito 2007; Casuccio et al. 2008; Domingo-Cabo et al. 2009; Belén et al. 2011) are shown in Fig. 19. From this figure it can be seen that Eq. (7) allows a better prediction of elastic modulus than those proposed in EC2 (Eq. (6)) for RAC. It can be pointed out also that the majority of experimental values are within the interval of ±10 % bounded by the two dotted red lines. Finally, it can be concluded that the relationship between E and f_c' does not seem affected by the nature of gravels.

EC2 proposes also a relation between the peak strain, ε_{c1}, to the compressive strength f_c' regardless the loading rate and the specimen size. This relation is given by the following expression:

$$\varepsilon_{c1} = 0.7\left(f_c'\right)^{0.31} \leq 2.8‰. \tag{8}$$

The validity of this expression was verified for 66 concretes of the literature with natural aggregates (see Table 8 in "Appendix" section). The results presented in Fig. 20 show that the previous expression of EC2 does not predicted well the peak strain. However, it can be shown that the proposed expression given by Eq. 9 is more suitable for the prediction of peak stain.

$$\varepsilon_{c1} = 1.1\left(f_c'\right)^{0.175}‰ \tag{9}$$

For the full stress–strain curve, EC2 proposes the simple following equation:

$$\frac{\sigma}{f_c'} = \frac{k\eta - \eta^2}{1 + (k-2)\eta}, \tag{10}$$

with $\eta = \varepsilon_c/\varepsilon_{c1}$, $k = 1.05 \times E_{cm}(\varepsilon_{c1}/f_c)$ and E_{cm} the secant modulus of elasticity. The model requires the knowledge of the static modulus of elasticity, the compressive strength and the peak strain ε_{c1}. The application of this model to recycled aggregates concrete shows that it does not reproduce suitably the post-peak behavior (Fig. 21). Another simple expression was proposed by Carreira and Chu (1985).

$$\frac{\sigma}{f_c'} = \frac{\beta\left(\frac{\varepsilon_c}{\varepsilon_{c1}}\right)}{\beta - 1 + \left(\frac{\varepsilon_c}{\varepsilon_{c1}}\right)^{\beta}}, \quad \text{with} \quad \beta = \frac{1}{1 - \frac{f_c'}{E\cdot\varepsilon_{c1}}} \tag{11}$$

Equations (7), (9) and (11) may therefore be used for the modeling of full stress–strain relationship of recycled aggregates concrete with the modification of peak strain with the replacement ratio. Figure 21 presents a comparison between the curves calculated using the modified model of Carreira and Chu (Eq. (9)) and the model of EC2 (Eq. (8)). It can be seen that this modified model is more adequate for the modeling of post-peak behavior as the model of EC2.

6. Conclusion

In this paper, a natural aggregates concrete, NAC, and three recycled concrete aggregates RAC30, RAC65 and RAC100 were prepared on the basis of an imposed constant flowability at fresh state and a target compressive strength of about 35 MPa at 28 days. Moreover only coarse aggregates were replaced by recycled ones with three volumetric replacement ratios being respectively 30, 65 and 100 %. Based on the experimental results the following conclusions can be drawn:

- The use of recycled aggregates up to 30 % does not affect the demand of water of concrete, but generates a reduction of 14 % of the compressive strength. By increasing the replacement ratio, the cement content increases to maintain constant W/C ratio causing an increase in the compressive strength which counterbalances the negative effect of recycled aggregates.
- Recycled aggregate concretes had lower elastic modulus, splitting and flexural tensile strength than normal aggregate one.
- The strain–stress curves under uniaxial compression show that the post-cracking branch is more spread out compared to NAC. In addition, the peak-strain increases by increasing the replacement ratio. These phenomena are explained by the more progressive and diffuse damage of concrete due to the presence of recycled aggregates.

New relationships for prediction of concrete's elastic modulus, and a peak strain from compressive strength were proposed. The predicted results for RAC were closer to experimental results than values predicted by equations proposed in EC2. For the complete strain–stress curve, a model based on the Carreira and Chu's model was proposed. The modified model is more adequate for the modeling of post-peak behavior than the model of EC2.

Open Access

Appendix: Database of Mechanical Characteristics

See Tables 7 and 8.

Table 7 Elastic modulus database.

Author	Nature of aggregates	Test conditions	Compressive strength (MPa)	Elastic modulus (MPa)
Ali et al. (1990)	Natural	Not communicated	16.7	13,820
			25.3	19,980
			27.7	23,530
			32.0	33,980
			43.5	44,550
Assié (2004)	Natural	Stress rate 0.5 MPa/s	22.6	28,400
			40.6	36,400
			55.1	38,200
			69.2	36,100
Belén et al. (2011)	Natural	Controlled load rate 8.77 kN/s	44.81	34,374
			31.92	30,645
	80 % natural + 20 % recycled		43.74	33,192
			31.71	29,598
	50 % natural + 50 % recycled		37.45	30,321
			32.35	27,459
	Recycled		40.54	24,817
			30.13	25,935

Table 7 continued

Author	Nature of aggregates	Test conditions	Compressive strength (MPa)	Elastic modulus (MPa)
El-Hilali (2009)	Natural	Stress rate 0.5 MPa/s	35.12	25,130
			42.12	32,660
			56.46	34,660
			60.84	37,660
			61.00	38,660
			77.95	48,850
			31.26	27,260
			38.18	33,660
			53.46	35,660
			59.31	39,660
			60.52	40,330
			75.21	51,260
			30.32	29,800
			36.68	35,330
			52.56	36,660
			55.72	40,330
			57.51	41,660
			71.95	53,230
Casuccio et al. (2008)	Natural	Stress rate	18.10	27,100
			37.50	33,100
			48.40	39,900
	Recycled		18.00	23,400
			36.40	28,800
			44.40	34,200
	Recycled		15.40	22,600
			35.70	28,300
			43.80	32,700
Cedolin and Cusatis (2008)	Natural	Not communicated	28.50	24,200
			33.70	32,680
			49.60	28,690
			54.80	28,600

Table 7 continued

Author	Nature of aggregates	Test conditions	Compressive strength (MPa)	Elastic modulus (MPa)
Wee et al. (1996)	Natural	Strain rate 0.07 mm/min	42.7	37,600
			63.2	41,800
			70.2	43,000
			65.1	41,500
			70.5	40,400
			69.7	41,500
			71.5	41,400
			63.6	42,600
			85.9	45,000
			90.2	44,400
			78.3	44,300
			85.9	44,300
			81.2	43,900
			88.1	44,500
			81.6	43,800
			82.6	44,200
			84.8	47,200
			85.6	45,600
			96.2	46,600
			46.4	35,200
			65.8	40,800
			73.9	41,600
			87.6	44,500
			93.1	45,400
			95.3	45,200
			100.6	45,800
			102.1	46,100
			102.8	46,700
			106.3	48,400
			104.2	46,300
			92.8	45,800
			94.6	47,300
			94	46,300
			96.6	46,500
			91.5	45,900
			93.6	47,100
			91.7	46,000
			119.9	49,100
			125.6	50,900

Table 7 continued

Author	Nature of aggregates	Test conditions	Compressive strength (MPa)	Elastic modulus (MPa)
Gesoglu et al. (2002)	Natural		77.2	47,100
			71.5	48,000
			66.5	46,800
			70.7	47,300
			61.8	45,400
			68.9	47,600
			59.1	40,900
			62.2	45,400
			75.8	43,000
			67.7	48,200
			53.6	46,200
			57.9	44,500
			92.9	46,400
			94	48,300
			97.7	47,000
			102	48,800
			93.7	50,500
			86.2	47,100
			87.9	43,000
			82.7	45,400
			79.1	44,700
			85.3	45,000
			86.9	46,100
			90.7	48,100
			89.5	47,600
			87.8	45,400
			90.3	45,000
			95.2	50,800
			92.2	50,000
			97.6	49,300
			87.5	48,500
			87.2	41,100
			80.4	43,200
			86.5	44,200
			83.9	44,300
			80.9	44,600
			84.5	45,300
			85.7	45,100

Table 7 continued

Author	Nature of aggregates	Test conditions	Compressive strength (MPa)	Elastic modulus (MPa)
Wu et al. (2001)	Natural	Not communicated	98.2	48,200
			70.4	39,500
			65.8	36,200
			60.5	31,500
			62.1	31,000
			44.8	37,500
			43.2	28,300
			46.6	30,100
			45.0	29,000
Shannag (2000)	Natural		68.0	38,500
			77.0	47,200
			86.0	43,800
			86.0	42,300
			89.5	38,600
			90.5	36,200
Baalbaki et al. (1991)	Natural		105.0	42,000
			106.0	44,000
			111.0	41,000
			99.3	45,000
			99.7	42,000
			95.3	40,000
			98.0	40,000
			103.0	40,000
			90.8	42,000
			89.2	41,000
Domingo-Cabo et al. (2009)	Natural	Not communicated	42.8	32,153
	20 % recycled + 80 % natural		42.7	31,178
	50 % recycled + 50 % natural		41.3	31,204
	Recycled		41.8	31,589
Fares (2009)	Natural	Stress rate 0.5 MPa/s	36.6	36,110
			52.7	39,000
			40.8	43,930
Etxeberria et al. (2007)	Natural	UNE 83-304-84	29.0	32,561,7
	25 % recycled + 75 % natural		28.0	31,300,4
	50 % recycled + 50 % natural		29.0	28,591,7
	Recycled		28.0	27,764

Table 7 continued

Author	Nature of aggregates	Test conditions	Compressive strength (MPa)	Elastic modulus (MPa)
Evangelista and de Brito (2007)	Natural	NP EN 12390-5	59.3	35,500
	30 % recycled + 70 % natural		57.1	34,200
	Recycled		54.8	28,900
Gomez-Soberon (2002)	Natural	Not communicated	39.0	29,700
	15 % recycled + 85 % natural		38.1	29,100
	30 % recycled + 70 % natural		37.0	27,800
	60 % recycled + 40 % natural		35.8	26,600
	Recycled		34.5	26,700
Karihaloo et al. (2006)	Natural	Not communicated	55.0	36,900
			60.0	38,300
			100.0	43,000
Kim et al. (1997, 2004)	Natural		18.5	26,772
			33.2	28,832
			58.0	35,794
			31.3	29,940
			47.4	33,720
			82.8	40,570
			32.6	28,790
			45.8	33,400
			85.7	39,570
			34.9	26,510
			55.3	31,580
			66.9	34,350
			88.8	38,140
Martínez-Lage et al. (2012)	Natural	Controlled strain rate 16 με/s	30.5	29,500
	50 % recycled +50 % natural		26.8	24,190
	Recycled		20.4	19,765
Zhao et al. (2008)	Natural	Not communicated	43.8	31,400
			43.4	39,200
			50.9	35,700
			56.4	35,900
			50.2	41,000
			50.8	38,900
			40.0	33,600
			51.7	39,600

Table 7 continued

Author	Nature of aggregates	Test conditions	Compressive strength (MPa)	Elastic modulus (MPa)
Dong and Keru (2001)	Natural	Not communicated	60.5	34,900
			60.5	32,700
			62.1	35,000
			83.6	44,900
			98.2	45,100
			63.0	39,800
			72.5	46,100
			77.4	38,500
			76.5	40,300
			70.2	42,800
			73.8	36,600
			75.1	38,600
			77.0	35,200
			76.8	39,700
			90.3	48,700
			91.2	42,600
			96.7	41,700
			85.5	42,100
			113.7	48,000
			35.9	29,600
			43.3	28,900
			45.8	34,700
			58.0	33,000
			59.7	34,000
Wardeh et al. (2010)	Natural	Strain rate 1 mm/min	46.5	35,000
Praveen et al. (2004)	Natural	Not communicated	36.7	27,527
			54.6	33,470
			70.8	37,614
Shen et al. (2009)	Natural	Loading rate 10 kN/s	28.6	25,130
			40.0	29,840
			57.9	32,040
			32.1	25,420
			42.2	26,000
			52.1	30,020
			48.8	27,800
			56.0	28,670
			68.8	33,030
Kang et al. (2014)	Natural	ASTM C39/C39 M	65.4	37,700
	15 % recycled + 85 % natural		59.4	36,200
	30 % recycled + 70 % natural		48.4	32,800
	Natural		38.6	29,200
	15 % recycled + 85 % natural		32.7	29,200
	30 % recycled + 70 % natural		31.7	26,500
	50 % recycled + 50 % natural		29	25,300

Table 8 strain at peak stress database.

Author	Nature of aggregates	Test conditions	Compressive strength (MPa)	Strain at peak stress
Belén et al. (2011)	Natural	Controlled strain rate 16 με/s	44.8	0.00190
			31.9	0.00174
	80 % natural + 20 % recycled		43.7	0.00189
			31.7	0.00199
	50 % natural + 50 % recycled		37.5	0.0019
			32.4	0.00195
	Recycled		40.5	0.00219
			30.1	0.00216
Martínez-Lage et al. (2012)	Natural	Controlled strain rate 16 με/s	30.5	0.0021
	50 % natural + 50 % recycled		26.8	0.0023
	Recycled		20.4	0.0025
Wee et al. (1996)	Natural	Strain rate 0.07 mm/min	63.2	0.00216
			70.2	0.0021
			65.1	0.00216
			70.5	0.00206
			69.7	0.00212
			71.5	0.00213
			63.6	0.00228
			85.9	0.00226
			90.2	0.00243
			78.3	0.00232
			85.9	0.00231
			81.2	0.00224
			88.1	0.00227
			81.6	0.00211
			82.6	0.00216
			84.8	0.00252
			85.6	0.00232
			96.2	0.00237
			73.9	0.00243
			87.6	0.00243
			93.1	0.00244
			95.3	0.00242
			100.6	0.00258
			102.1	0.00256
			102.8	0.00247
			106.3	0.00251
			104.2	0.00249
			92.8	0.00242
			94.6	0.00228
			96.6	0.00232
			91.5	0.00228
			93.6	0.00219
			91.7	0.00266
			119.9	0.00275
			125.6	0.00273

Table 8 continued

Author	Nature of aggregates	Test conditions	Compressive strength (MPa)	Strain at peak stress
Dhonde et al. (2007)	Natural	Stress rate 0.25 MPa/s	31.2	0.00147
			38.5	0.00178
			50.5	0.00194
			77.6	0.00191
Praveen et al. (2004)	Natural	Not communicated	36.7	0.002
			54.6	0.0023
			70.8	0.0025
Ali et al. (1990)	Natural	Not communicated	16.7	0.0018
			25.3	0.0021
			27.7	0.0021
			32.0	0.0022
			43.5	0.0022
Prasad et al. (2009)	Natural	Strain rate	23.3	0.00197
			39.6	0.00235
Suresh Babu et al. (2008)	Natural	Strain rate	25.0	0.001905
			31.0	0.00207
			31.5	0.00209
			25.8	0.00199
			28.0	0.00203
Carreira and Chu (1985)	Natural	Not communicated	20.7	0.0018
			30.5	0.0018
			49.5	0.00195
Carreira and Chu (1985)	Natural	Not communicated	10.7	0.0015
			20.0	0.0019
			34.8	0.0022
			46.9	0.0021
			52.4	0.00195

References

Ali, A. M., Farid, B., & Al-Janabi, A. I. M. (1990). Stress–strain relationship for concrete in compression model of local materials. *Journal of King Abdulaziz University: Engineering Sciences, 2*, 183–194.

Assié, S. (2004). *Durability of self compacting concretes* (254 pp). PhD Thesis, INSA-Toulouse, Toulouse (in French).

Baalbaki, W., Benmokrane, B., Chaallal, O., & Aitcin, P.-C. (1991). Influence of coarse aggregate on elastic properties of high-performance concrete. *ACI Materials Journal, 88*(5), 499–503.

Belén, G.-F., Fernando, M.-A., Carro Lopez, D., & Seara-Paz, S. (2011). Stress–strain relationship in axial compression for concrete using recycled saturated coarse aggregate. *Construction and Building Materials, 25*(5), 2335–2342.

Belin, P., Habert, G., Thiery, M., & Thiery, M. (2013). Cement paste content and water absorption of recycled concrete coarse aggregates. *Materials and Structures*, 1–15. doi: 10.1617/s11527-013-0128-z.

Carreira, D. J., & Chu, K.-H. (1985). Stress–strain relationship for plain concrete in compression. *ACI Materials Journal, 82*(6), 797–804.

Casuccio, M., Torrijos, M.-C., Giaccio, G., & Zerbino, R. (2008). Failure mechanism of recycled aggregate concrete. *Construction and Building Materials, 22*(7), 1500–1506.

Cedolin, L., & Cusatis, G. (2008). Identification of concrete fracture parameters through size effect experiments. *Cement & Concrete Composites, 30*(9), 788–797.

de Juan, M.-S., & Gutirrez, P.-A. (2009). Study on the influence of attached mortar content on the properties of recycled concrete aggregate. *Construction and Building Materials, 23*(2), 872–877.

Dhonde, H.-B., Mo, Y.-L., Hsu, T. T.-C., & Vogel, J. (2007). Fresh and hardened properties of self-consolidating fiber-reinforced concrete. *ACI Journal, 104*(5), 491–500.

Djerbi Tegguer, A. (2012). Determining the water absorption of recycled aggregates utilizing hydrostatic weighing approach. *Construction and Building Materials, 27*(1), 112–116.

Domingo-Cabo, A., Lazaro, C., Lopez-Gayarre, F., Serrano-Lopez, M. A., Serna, P., & Castano-Tabares, J. O. (2009). Creep and shrinkage of recycled aggregate concrete. *Construction and Building Materials, 23*(7), 2545–2553.

Dong, Z., & Keru, W. (2001). Fracture properties of high-strength concrete. *Journal of Materials in Civil Engineering, 13*(1), 86–88.

El-Hilali, A. (2009). *Experimental study of the rheology and the behaviour and self-compacting concrete (SCC): Influence of limestone filler and vegetable fibres* (p. 200). PhD Thesis, University of Cergy-Pontoise (in French).

Etxeberria, M., Vazquez, E., Mari, A., & Barra, M. (2007). Influence of amount of recycled coarse aggregates and production process on properties of recycled aggregate concrete. *Cement and Concrete Research, 37*(5), 735–742.

Evangelista, L., & de Brito, J. (2007). Mechanical behaviour of concrete made with fine recycled concrete aggregates. *Cement & Concrete Composites, 29*(5), 397–401.

Fares, H. (2009). *Mechanical and physico-chemical properties of self compacting concrete exposed to heigh temperatures* (p. 206). PhD Thesis, University of Cergy-Pontoise (in French).

Gesoglu, M., Güneyisi, E., & Özturan, T. (2002). Effects of end conditions on compressive strength and static elastic modulus of very high strength concrete. *Cement and Concrete Research, 32*(10), 1545–1550.

Gomes, M. & de Brito, J. (2009). Structural concrete with incorporation of coarse recycled concrete and ceramic aggregates: durability performance. *Materials and Structures, 42*(5), 663–675. doi:10.1617/s11527-008-9411-9).

Gomez-Soberon, J. M. V. (2002). Porosity of recycled concrete with substitution of recycled concrete aggregate: An experimental study. *Cement and Concrete Research, 32*(8), 1301–1311.

Hacene, S.-M.-A. B., Ghomari, F., Schoefs, F., & Khelidj, A. (2009). Etude expérimentale et statistique de l'influence de l'affaissement et de l'air occlus sur la résistance a la compression des bétons. *Lebanese Science Journal, 10*(2), 81–100.

Hansen, T. C., & Boegh, E. (1986). Elasticity and drying shrinkage of recycled aggregate concrete. *ACI Journal, 82*(5), 648–652.

Julio, E., Dias, N., Lourenço, J., & Silva, J. (2006). Feret coefficients for white self-compacting concrete. *Materials and Structures, 39*(5), 585–591. doi:10.1007/s11527-005-9048-x.

Kang, T. H.-K., Kim, W., Kwak, Y.-K., & Hong, S.-G. (2014). Flexural testing of reinforced concrete beams with recycled concrete aggregates. *ACI Structural Journal*, *111*(3), 607–616.

Karihaloo, B.-L., Abdalla, H.-M., & Xiao, Q.-Z. (2006). Deterministic size effect in the strength of cracked concrete structures. *Cement and Concrete Research, 36*(1), 171–188.

Kim, J.-K., Lee, C.-S., Park, C.-K., & Eo, S.-H. (1997). The fracture characteristics of crushed limestone sand concrete. *Cement and Concrete Research, 27*(11), 1719–1729.

Kim, J.-K., Lee, Y., & Yi, S.-T. (2004). Fracture characteristics of concrete at early ages. *Cement and Concrete Research, 34*(3), 507–519.

Kou, S.-C., Poon, C.-S., & Etxeberria, M. (2011). Influence of recycled aggregates on long term mechanical properties and pore size distribution of concrete. *Cement & Concrete Composites, 33*(2), 286–291.

Lédée, M. V., de Larrard F., Sedran, T., & Brochu, F.-P. (2004). *Essai de compacité des fractions granulaires à la table à secousses—Mode opératoire*. M. d. e. no. 61 (p. 13). Paris, France Laboratoire Central des Ponts et Chaussées (in French).

Li, X. (2008). Recycling and reuse of waste concrete in China: Part I. Material behaviour of recycled aggregate concrete. *Resources, Conservation and Recycling 53*(1–2), 36–44.

Manzi, S., Mazzotti, C., & Bignozzi, M. C. (2013). Short and long-term behavior of structural concrete with recycled concrete aggregate. *Cement & Concrete Composites, 37*, 312–318.

Martinez-Lage, I., Martinez-Abella, F., Vazquez-Herrero, C., & Perez-Ordonez, J.-L. (2012). Properties of plain concrete made with mixed recycled coarse aggregate. *Construction and Building Materials, Non Destructive Techniques for Assessment of Concrete, 37*, 171–176.

McNeil, K. & Kang T.-K. (2013). Recycled concrete aggregates: A review. *International Journal of Concrete Structures and Materials, 7*(1), 61–69 doi:10.1007/s40069-013-0032-5).

Pereira, P., Evangelista, L., & de Brito, J. (2012). The effect of superplasticisers on the workability and compressive strength of concrete made with fine recycled concrete aggregates. *Construction and Building Materials, 28*(1), 722–729.

Poon, C.-S., Kou S.-C., & Lam, L. (2007). Influence of recycled aggregate on slump and bleeding of fresh concrete. *Materials and Structures, 40*(9), 981–988. doi: 10.1617/s11527-006-9192-y.

Prasad, M. L. V., Rathish Kumar, P., & Oshima, T. (2009). Development of analytical stress–strain model for glass fiber self compacting concrete. *International Journal of Mechanics and Solids, 4*(1), 25–37.

Praveen, K., Haq, M.-A., & Kaushik, S.-K. (2004). Early age strength of SCC with large volumes of fly ash. *Indian concrete Journal, 78*(6), 25–29.

Sedran, T. (1999). *Rhéologie et Rhéométrie des bétons: Application aux bétons autonivelants* (p. 220). Champs-sur-Marne: Ecole nationale des Ponts et Chaussées.

Shannag, M. J. (2000). High strength concrete containing natural pozzolan and silica fume. *Cement & Concrete Composites, 22*(6), 399–406.

Shen, J., Yurtdas, I. Diagana, G., & Li, A. (2009). Evolution of the uniaxial mechanical behavior of self-compacting concrete (SCC): Effect of the compressive strength. In *27th meeting of civil engineering universities*, St. Malo, France.

Suresh Babu, T., Seshagiri Rao, M. V., & Rama Seshu, D. (2008). Mechanical properties and stress–strain behavior of self compacting concrete with and without glass fibres. *Asian Journal of Civil Engineering (Building and Housing), 9*(5), 457–472.

Tam, V. W.-Y., Gao, X. F., Tam, C. M., & Chan, C. H. (2008). New approach in measuring water absorption of recycled aggregates. *Construction and Building Materials, 22*(3), 364–369.

UNICEM L'Union nationale des industries de carrières et matériaux de construction. Reteieved, from http://www.unicem.fr/. Accessed 2013.

UNPG Union Nationale des Producteurs de Granulats. Reteieved, from http://www.unpg.fr/. Accessed 2013.

Wardeh, G., Ghorbel, E., & Mignot, V. (2010). *Fracture properties of hybrid fibre self compacting concrete* (pp. 219–224). Marianske Lazne: Concrete structures for challenging times.

Wee, T., Chin, M., & Mansur, M. (1996). Stress–strain relationship of high-strength concrete in compression. *Journal of Materials in Civil Engineering, 8*(2), 70–76.

Wu, K.-R., Chen, B., Yao, W., & Zhang, D. (2001). Effect of coarse aggregate type on mechanical properties of high-performance concrete. *Cement and Concrete Research, 31*(10), 1421–1425.

Xiao, J., Li, J., & Zhang, C. (2005). Mechanical properties of recycled aggregate concrete under uniaxial loading. *Cement and Concrete Research, 35*(6), 1187–1194.

Xiao, J., Sun, Y., & Falkner, H. (2006). Seismic performance of frame structures with recycled aggregate concrete. *Engineering Structures, 28*(1), 1–8.

Zhao, Z., Kwon, S.-H., & Shah, S.-P. (2008). Effect of specimen size on fracture energy and softening curve of concrete: Part I. Experiments and fracture energy. *Cement and Concrete Research, 38*(8–9), 1049–1060.